Evaluation of Gynecologic Cancer with MR Imaging, ^{18}F-FDG PET/CT, and PET/MR Imaging

Susanna I. Lee[1], Onofrio A. Catalano[2], and Farrokh Dehdashti[3]

[1]Department of Radiology, Massachusetts General Hospital, Harvard Medical School, Boston, Massachusetts; [2]Department of Radiology, University of Naples Parthenope and SDN Istituto Ricerca Diagnostica Nucleare, Naples, Italy; and [3]Department of Nuclear Medicine, Mallinckrodt Institute of Radiology, Washington University, St. Louis, Missouri

Learning Objectives: On successful completion of this activity, participants should be able to (1) explain the complementary role of pelvic MR imaging and ^{18}F-FDG PET/CT in the care of gynecologic cancer patients; (2) assess the application of functional MR imaging techniques and PET tracers under development to gynecologic cancer imaging; and (3) recognize the potential of PET/MR imaging as a modality that can integrate the gynecologic cancer imaging work-up.

Financial Disclosure: The authors of this article have indicated no relevant relationships that could be perceived as a real or apparent conflict of interest.

CME Credit: SNMMI is accredited by the Accreditation Council for Continuing Medical Education (ACCME) to sponsor continuing education for physicians. SNMMI designates each *JNM* continuing education article for a maximum of 2.0 AMA PRA Category 1 Credits. Physicians should claim only credit commensurate with the extent of their participation in the activity. For CE credit, SAM, and other credit types, participants can access this activity through the SNMMI website (http://www.snmmilearningcenter.org) through March 2018.

MR imaging and ^{18}F-FDG PET/CT play central and complementary roles in the care of patients with gynecologic cancer. Because treatment often requires combinations of surgery, radiotherapy, and chemotherapy, imaging is central to triage and to determining prognosis. This article reviews the use of the 2 imaging modalities in the initial evaluation of 3 common cancers: uterine cervical, uterine endometrial, and epithelial ovarian. Imaging features that affect management are highlighted, as well as the relative strengths and weaknesses of the 2 modalities. Use of imaging after initial therapy to assess for recurrence and to plan salvage therapy is described. Newer functional and molecular techniques in MR imaging and PET are evaluated. Finally, we describe our initial experience with PET/MR imaging, an emerging technology that may prove to be a mainstay in personalized gynecologic cancer care.

Key Words: Cu-labeled diacetyl-bis (N4-methylthiosemicarbazone) PET; 16α-^{18}F-fluoro-17β-estradiol PET; diffusion weighted imaging; dynamic contrast enhanced MRI; perfusion MRI

J Nucl Med 2015; 56:436–443
DOI: 10.2967/jnumed.114.145011

Gynecologic cancers are classified according to their anatomic site of origin and include cancers of the ovaries and fallopian tubes, uterine corpus, uterine cervix and vagina, and vulva. Multidisciplinary approaches that combine surgery, chemotherapy, and radiotherapy are often used, and imaging plays a central role in treatment planning, in triaging patients, in define the scope of the disease, and in evaluating the success of therapy.

Received Oct. 27, 2014; revision accepted Dec. 15, 2014.
For correspondence or reprints contact: Susanna I. Lee, Massachusetts General Hospital, 55 Fruit St., White 270, Boston, MA 02114.
E-mail: slee0@partners.org
Published online Jan. 29, 2015.

This article reviews the role of imaging in the management of the 3 most common cancers, that is, uterine cervical, uterine endometrial, and epithelial ovarian. The complementary roles of MR imaging and integrated PET/CT with ^{18}F-FDG both at primary presentation and after treatment are discussed (Table 1). MR imaging techniques and PET tracers in development that show promise for clinical application are presented. Finally, the potential use of PET/MR imaging, an emerging technology, is summarized.

UTERINE CERVICAL CANCER

Worldwide, cervical cancer is the leading cause of cancer-related death in women. In the United States, disease incidence and mortality have declined significantly because of routine screening, with 12,360 new diagnoses and 4,020 deaths being projected for 2014 (*1*). The International Federation of Gynecology and Obstetrics (FIGO) system stages cervical cancer clinically (Supplemental Table 1; supplemental materials are available at http://jnm.snmjournals.org) on the basis of physical examination, cystoscopy, proctoscopy, colposcopy, and biopsy (*2*). Imaging is not described, although its use is implied in the detection of hydronephrosis (stage IIIB) and distant metastases (stage IVB). The National Cancer Comprehensive Network (NCCN) practice guidelines for cervical cancer work-up include chest radiography, CT or PET/CT, and MR imaging as indicated (*3*).

At presentation, the most common treatment choice to be made is between surgery and concurrent chemoradiotherapy. Each alone is potentially curative, with surgery reserved for small (<4 cm) local tumors (stages IA, IB1, and IIA1). Imaging findings that usually triage a patient to chemoradiation are tumor size and parametrial extension, best seen on MR imaging (Fig. 1), and lymphadenopathy, best seen on ^{18}F-FDG PET/CT (Table 1). The choice of optimal primary therapy that minimizes morbidity is best achieved when both MR imaging and ^{18}F-FDG PET/CT are included in the pretreatment work-up (*4*).

An intergroup multicenter study in the United States showed that, in patients with early-stage tumor intended for curative radical hysterectomy, sensitivity and specificity for detecting

TABLE 1
Imaging in Tumor Assessment Preceding and Following Primary Therapy

Parameter	MR imaging	^{18}F-FDG PET/CT
Uterine cervical cancer: pretreatment		
Early detection	Poor	Poor
Differential diagnosis (benign vs. malignant)	Possible	Poor
Extent of tumor spread		
Tumor size	Best	Poor
Endocervical margin distance	Best	Poor
Parametrial involvement	Best	Possible
Lower-third-of-vagina involvement	Possible	Poor
Pelvic sidewall involvement	Possible	Possible
Hydronephrosis	Possible	Possible
Bladder mucosal involvement	Possible	Poor
Rectal mucosal involvement	Possible	Poor
Pelvic and paraaortic lymphadenopathy	Possible	Best
Distant metastases (lymph nodes and bone)	Possible	Best
Distant metastases (liver)	Best	Possible
Distant metastases (lung)	Poor	Possible
Uterine cervical cancer: posttreatment		
Local or regional surveillance or suspected recurrence	Best	Possible
Whole-body surveillance or suspected recurrence	Possible	Best
Uterine endometrial cancer: pretreatment		
Early detection	Poor	Poor
Differential diagnosis (benign vs. malignant)	Possible	Possible
Extent of tumor spread		
Greater than half thickness of myometrium extension	Best	Possible
Cervical stromal involvement	Best	Possible
Uterine serosal or adnexal involvement	Best	Possible
Vaginal or parametrial involvement	Best	Possible
Pelvic and paraaortic adenopathy	Possible	Best
Bladder mucosal involvement	Possible	Poor
Bowel mucosal involvement	Possible	Poor
Distant metastases (lymph nodes and bone)	Possible	Best
Distant metastases (liver)	Best	Possible
Distant metastases (lung)	Poor	Possible
Uterine endometrial cancer: posttreatment		
Local surveillance or suspected recurrence	Best	Possible
Whole-body surveillance or suspected recurrence	Possible	Best
Ovarian cancer: pretreatment		
Early detection	Poor	Poor
Differential diagnosis (benign vs. malignant)	Best	Poor
Extent of tumor spread		
Ovary confined	Best	Poor
Pelvis confined	Possible	Possible
Abdominal involvement	Possible	Possible
Retroperitoneal adenopathy	Possible	Best
Peritoneal or pleural effusion	Possible	Poor
Distant metastases (lymph nodes and bone)	Possible	Best
Distant metastases (intraparenchymal liver)	Best	Possible
Distant metastases (lung)	Poor	Possible
Ovarian cancer: posttreatment		
Local or regional surveillance or suspected recurrence	Best	Possible
Whole-body surveillance or suspected recurrence	Possible	Best

Poor = poor modality choice or insufficient data; best = best modality choice; possible = possible modality choice.
Comparative assessment of modality includes clinical options, such as pelvic examination and optical imaging (e.g., colposcopy, cystoscopy, or proctoscopy), with biopsy.

disease higher than stage IIB (i.e., parametrial tumor extension) are 53% and 75%, respectively, with MR imaging and 29% and 99%, respectively, with clinical assessment (*5*). For measuring tumor size, MR imaging was shown to be superior to CT or clinical examination (*6*). Lymphadenopathy, although not included in the FIGO staging system, is the major factor driving treatment planning and is the best indicator of prognosis. For patients with clinically visible tumor, ^{18}F-FDG PET/CT is more sensitive than either CT or MR imaging in the evaluation of nodal involvement (Table 2) (*7–9*). Studies using histopathology as the gold standard have shown that ^{18}F-FDG PET and ^{18}F-FDG PET/CT have a fairly wide range of sensitivity (65%–86%) and high specificity (94%–97%) for lymph node detection in patients with advanced-stage cervical cancer without evidence of node metastasis on anatomic imaging (*10,11*). Currently, ^{18}F-FDG PET/CT is routinely used for radiation therapy planning. In addition, the extent of lymph node involvement on ^{18}F-FDG PET and PET/CT has been shown to be a strong predictor of disease-specific survival (Fig. 2). The risk of disease recurrence increases incrementally on the basis of the most distant level of PET lymph node involvement, with a hazard ratio of 2.40 (95% confidence interval, 1.63–3.52) for pelvic, 5.88 (3.80–9.09) for paraaortic, and 30.27 (16.56–55.34) for supraclavicular involvement (*12*).

Radical trachelectomy and lymphadenectomy is a fertility-sparing treatment option for women with early-stage disease. Eligibility requirements include tumor smaller than 2 cm, distance from tumor margin to internal cervical os of more than 1 cm, and absence of lymph node metastases. MR imaging assesses the extent of local tumor with high accuracy (*13*) and is routinely used for patient selection. ^{18}F-FDG PET/CT is also used in many institutions to evaluate for lymphadenopathy. But because the test demonstrates low (32%) sensitivity in early-stage disease, its purpose is to identify ineligible candidates (*14*). Surgical lymphadenectomy is performed on all patients undergoing fertility-sparing surgery, even in the absence of imaging evidence of lymph node metastases.

After treatment, disease will recur in approximately one third of patients treated for locally advanced cancer, and most of these recurrences will be within the first 2 y after initial therapy. Because ^{18}F-FDG PET results have been shown to be prognostic of patient survival, the NCCN guidelines state that a single PET/CT examination can be performed 3–6 mo after chemoradiation (Table 1). Patients with new, residual, or no disease on posttreatment imaging demonstrate 5-y survival rates of 0%, 46%, and 92%, respectively (*15*). MR imaging is not routinely used in the posttreatment setting.

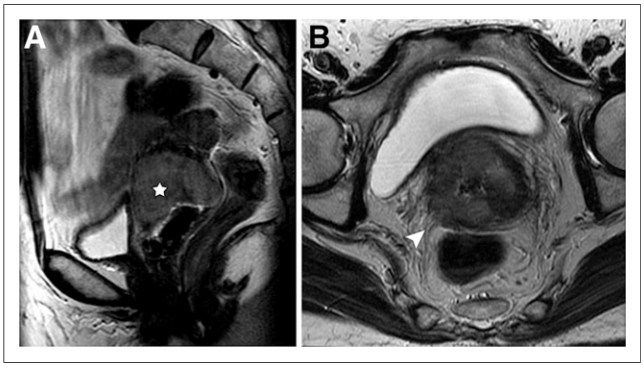

FIGURE 1. MR imaging of cervical cancer with parametrial extension. Fast spin echo T2-weighted sagittal image (A) shows 4.3-cm solid intermediate-signal tumor (star) that, on axial image (B), invades radially out of cervix into adjacent right parametria (arrowhead).

UTERINE ENDOMETRIAL CANCER

Endometrial cancer is the most commonly diagnosed gynecologic malignancy in the United States, with 52,630 new cases of uterine corpus cancer and 8,590 deaths predicted in 2014 (*1*). Patients typically present with abnormal vaginal bleeding early in the course of disease, are screened with transvaginal pelvic ultrasound, and are diagnosed with endometrial biopsy. The FIGO system stages endometrial cancer surgically (Supplemental Table 1) (*2*), and imaging is not described. The NCCN guidelines for endometrial cancer work-up specify chest imaging and also mention MR imaging, CT, and ^{18}F-FDG PET as possible options to consider in patients suspected to have extrauterine disease (*16*). A European imaging society recommends MR imaging for treatment planning (*17*). The wide latitude provided in the consensus guidelines on pretreatment imaging for endometrial cancer reflects the variability in practice among institutions.

Hysterectomy and bilateral salpingo-oophorectomy is the first step in treatment of endometrial cancer patients presumed to be at stages I–III. Surgery can also include resection of the pelvic and paraaortic nodes to assess for lymphadenopathy, which is part of the staging criteria. Because lymphadenectomy can incur perioperative complications and long-term morbidity such as lymphedema, some centers have chosen to selectively perform the procedure only when the primary tumor demonstrates high-risk features. These are high-grade histology (grade 3 endometrioid, serous papillary, or clear cell adenocarcinomas), a tumor larger than 2 cm, deep (>50% thickness) myometrial invasion, or cervical stromal invasion (*18*). If preoperative evaluation indicates likely stage IV cancer spread, curative surgical resection is not an option and the patient can be offered compassionate triage to chemotherapy and, if necessary, surgery for palliation.

Pretreatment imaging is obtained to plan surgery (Table 1). Because features of the primary tumor predict the likelihood of nodal metastases, sites with expertise in frozen section diagnosis often choose to forego imaging and make the decision to perform lymphadenectomy intraoperatively, based on the hysterectomy specimen. However, many institutions, especially in Western Europe and Asia, opt for preoperative MR imaging to determine whether lymphadenectomy will likely be required. In a multicenter audit of 775 cases over a 12-mo period in the United Kingdom, MR imaging demonstrated sensitivity and specificity of 77% and 88%, respectively, for detecting deep myometrial invasion; 42% and 97%, respectively, for detecting cervical stromal invasion; and 64% and 96%, respectively, for diagnosing pelvic lymphadenopathy (*19*). PET/CT is more sensitive than CT or MR imaging for directly evaluating for nodal metastases (Table 2) and is useful for identifying tumor-involved nodes for surgical resection (*20–22*). Nevertheless, because the sensitivity of PET/CT is suboptimal in detecting small-volume disease, staging lymphadenectomy is still performed in patients without imaging evidence of extrauterine disease when the primary tumor demonstrates high-risk features.

Imaging is also used in the minority of patients for whom staging surgery is not indicated as the initial treatment choice.

TABLE 2
Diagnostic Performance in Detection of Lymphadenopathy from Uterine Cancer

Modality	Sensitivity	Specificity
CT, cervical (*5,9*)	31%–57%	92%–97%
CT, endometrial (*22*)	28%–64%	78%–94%
MR imaging, cervical (*5,9*)	37%–55%	93%–94%
MR imaging, endometrial (*20,22*)	59%–72%	93%–97%
PET/CT, cervical (*7,8*)	72%–75%	96%–100%
PET/CT, endometrial (*20,21*)	74%–77%	93%–100%

Between 3% and 5% of patients with high-grade tumor histology harbor disease beyond the uterus and abdominopelvic nodes, such as intrathoracic or bony metastases (stage IVB). Thus, in patients for whom biopsy demonstrates high-risk histology, PET/CT is used to identify unsuspected distant disease that would obviate the morbidity of a staging operation (*23*). In patients with medical comorbidities that preclude surgery or those with tumor invading the bladder or bowel (stage IVA), MR imaging is obtained to delineate fields for radiotherapy, which constitutes an alternative initial therapy.

Most patients are cured after primary treatment, with 20%–25% developing recurrence, usually within the first 3 y. The majority of the recurrences are in patients with higher-risk tumors and with a 5% recurrence rate for those with stage I tumor. The most common sites for recurrent tumor are the lymph nodes, best assessed with PET/CT (Fig. 3), and the vagina, best assessed on physical examination and biopsy. Whole-body PET or integrated PET/CT demonstrates 92%–93% sensitivity and 93%–100% specificity in detecting recurrent disease (*24,25*). Surveillance imaging in patients at high risk for recurrence has been suggested, as 20% present with clinically occult metastases (*26*); but this use remains controversial.

OVARIAN CANCER

Ovarian cancer is the leading cause of gynecologic cancer deaths in Western countries. In the United States, 21,980 new diagnoses and 14,270 deaths were projected for 2014. A classification system based on pathologic and genetic features defines 2 types of epithelial ovarian cancer (*27*). Type I (25%) includes low-grade serous, low-grade endometrioid, clear cell, and mucinous tumors; is usually confined to the ovary at diagnosis; and demonstrates an indolent clinical course. Type II (75%) includes high-grade serous, high-grade endometrioid, and undifferentiated carcinomas, typically present as stage III or IV disease and accounting for 90% of ovarian cancer deaths.

Ovarian cancer is diagnosed clinically on the basis of patient history, imaging, and serum tumor markers (CA-125) and confirmed histologically. Early diagnosis, in the phase when the tumor is ovary-confined and likely curable, remains a challenge. Screening trials using transvaginal pelvic ultrasound have proven ineffective, in part because of the low prevalence of tumor in the background of benign ovarian masses. In one trial of 25,327 women over age 50 y, 1.5% of ovarian cancer was noted among a 19.6% incidence of benign cysts (*28*). In this context, MR imaging, demonstrating 81% sensitivity and 98% specificity for cancer detection, is used to characterize incidental ovarian masses and improve the positive predictive value of the imaging work-up (Table 1) (*29*). In contrast, ^{18}F-FDG PET, demonstrating 58% sensitivity and 76% specificity, is not advised (*30*).

The FIGO system stages ovarian cancer on the basis of findings at cytoreductive surgery and biopsy (Supplemental Table 1) (*31*). Prognosis is directly related to the successful resection of all visible tumor. Hence, standard treatment involves aggressive surgery followed by platinum- and taxane-based chemotherapy. Neoadjuvant chemotherapy followed by interval surgery is chosen for patients with medical comorbidities or with a tumor burden that is not amenable to complete resection.

Pretreatment imaging is used to define tumor extent and identify patients for whom primary surgery is unlikely to be successful. NCCN guidelines include abdominopelvic CT or MR imaging in this context (*32*). A multicenter trial of 280 patients with advanced ovarian cancer reported equal accuracy for CT and MR imaging (area under the curve [AUC], 0.96 for both) for diagnosis of intraperitoneal tumor implants (*33*). Because CT is more widely available, is better tolerated, and yields higher-resolution anatomic information, it is the chosen modality at most institutions. Although fusion PET/CT shows higher staging accuracy, mostly by identifying extraabdominopelvic disease, it has not

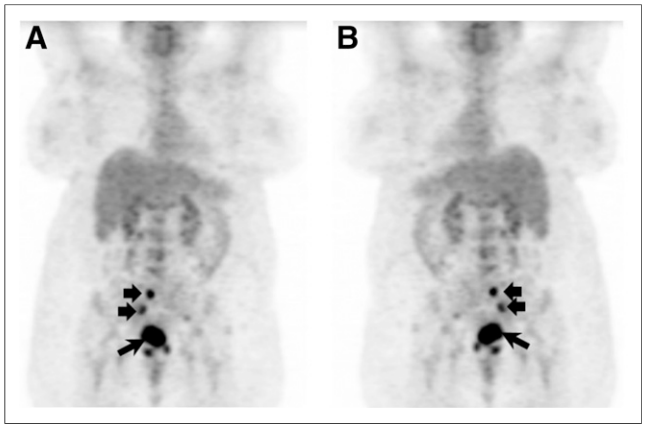

FIGURE 2. ^{18}F-FDG PET of cervical cancer lymphadenopathy. Anterior (A) and posterior (B) reprojection images demonstrate intense tracer uptake within known primary cervical carcinoma (long arrow) and right pelvic lymph node metastases (short arrows).

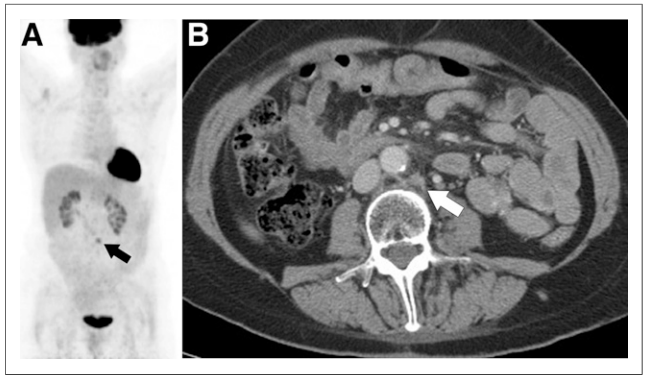

FIGURE 3. ^{18}F-FDG PET/CT of recurrent endometrial cancer. Coronal PET image (A) demonstrates focus of uptake in mid abdomen (arrow) corresponding to normal-sized paraaortic node (arrow) on diagnostic CT (B). Biopsy confirmed recurrent tumor.

been widely adopted, as evidence that this capability alters treatment is lacking.

Although most patients will respond to primary therapy, 60%–70% will eventually relapse, and almost all of them will die from their disease.

Surveillance involves physical examination and serial serum CA-125 measurements in most patients. Imaging is reserved for those in whom recurrence is suspected. In this setting, PET/CT (AUC, 0.96) demonstrates better diagnostic performance than CT (AUC, 0.88) or MR imaging (AUC, 0.80) (Table 1) (*34*) and better interpreter agreement than CT (*35*).

MR IMAGING TECHNOLOGIES IN DEVELOPMENT

Several newer MR imaging techniques show potential to add to the capability of MR imaging in lesion detection and characterization. These include dynamic contrast-enhanced (DCE) imaging, diffusion-weighted imaging (DWI), intrinsic susceptibility-weighted or blood oxygen level–dependent imaging, and proton spectroscopy. The latter two are primarily investigational tools. In contrast, standard protocols for evaluating the female pelvis routinely include DCE MR imaging and DWI. Research has focused on developing these methods as imaging biomarkers.

DCE MR imaging measures the kinetic profile of an intravenously injected bolus of gadolinium contrast as it passes from the neovascularity within the tumor into the extracellular space, thereby modeling tumor perfusion. Quantitative results are obtained by directly measuring descriptive data, such as initial area under the gadolinium curve, or by applying a pharmacokinetic mathematic model (*36*) to generate physiologic parameters, such as the volume of the extracellular, extravascular leakage space.

DCE MR imaging is routinely performed qualitatively in endometrial cancer patients to diagnose deep myometrial invasion, where it demonstrates 77%–88% sensitivity and 61%–100% specificity (*37,38*). Quantitative DCE MR imaging parameters have been reported to predict the outcome of cervical cancer radiotherapy (*39*) and to aid in discriminating benign from malignant adnexal masses (*40*). These results, if verified by independent investigators, would represent useful tools for development of adaptive therapy and noninvasive diagnosis, respectively.

DWI measures the Brownian motion of extracellular water and thereby approximates tissue cellularity and fluid viscosity. A series of pulse sequences incrementally weighted to diffusion is acquired by successively altering the amplitude, duration, and spacing of magnetic field gradients. These gradients spoil the signal from moving protons, accentuating the signal from protons slowed by cell packing or high fluid viscosity. The apparent diffusion coefficient (ADC) is a quantitative parameter derived from the exponential attenuation of signal between at least 2 acquisitions with different amounts of diffusion weighting. Restricted diffusion is depicted as high signal on the index diffusion-weighted images and low signal in the corresponding ADC maps. Thus, DWI provides concurrent lesion detection over a large field of view and quantitative tissue characterization.

Malignant tissue demonstrates restricted diffusion, that is, low ADC values, which normalize after therapy. As the increase in ADC values precedes decreased morphologic size, ADC values measured early during the course of therapy have been studied as a possible predictive biomarker. In a series of 111 patients with endometrial cancer, a multivariate analysis showed that the pretreatment minimal ADC of the primary tumor was an independent prognostic factor of disease recurrence ($P = 0.019$) (*41*). Such results suggest that quantitative DWI should be further explored as an early biomarker for adaptive therapy.

Aside from tissue characterization, DWI is routinely incorporated in clinical protocols to facilitate lesion detection. The contrast in signal between bright tumor against the relatively dark normal tissue seen on diffusion-weighted images improves conspicuity. The extent of peritoneal carcinomatosis (Fig. 4) (*42*) and intrauterine tumor spread (*38,43*) is more accurately assessed with DWI. In detection of lymphadenopathy, DWI when combined with conventional MR imaging has been shown to improve accuracy in some series (*44,45*) and not in others (*46*). Whole-body DWI (Fig. 5) is an emerging technique that allows for complete anatomic staging and detection of distant metastases (*47*).

PET TRACERS IN DEVELOPMENT

Several PET tracers have shown promise in evaluating specific biologic features and clinical behavior of gynecologic cancers. One example is copper-labeled diacetyl-bis (N4-methylthiosemicarbazone) (copper-ATSM), which measures hypoxia. Tumor hypoxia is an important prognostic factor indicating decreased overall and disease-free survival in patients with cervical cancer (*48,49*). The gold standard for measuring hypoxia is oxygen electrodes. However, this method is subject to sampling error and is practically available only in readily accessible tumors. copper-ATSM is a neutral lipophilic molecule that diffuses from the blood to the surrounding cells. Once intracellular, it undergoes reduction and becomes trapped and accumulates avidly in hypoxic cells but washes out rapidly from normoxic cells without any change. ATSM has been labeled using several radioisotopes of copper; however, most commonly ^{60}Cu (23.4-min half-life, $\beta+ = 81\%$), ^{62}Cu (9.7-min half-life, $\beta+ = 97.5\%$), and ^{64}Cu (12.7-h half-life, $\beta+ = 17\%$, $\beta- = 40\%$) have been used for clinical studies (*50*). Several studies on patients with cervical cancer have shown that ^{60}Cu-ATSM uptake is predictive of survival; cause-specific and overall survival were significantly worse in patients with increased pretreatment copper-ATSM uptake within the primary tumor (*51,52*). In addition, tumor uptake of ^{18}F-FDG in these patients did not correlate with copper-ATSM uptake, as no significant difference was found in tumor ^{18}F-FDG uptake between patients with hypoxic (ATSM-avid) tumors and patients who had normoxic tumors. Thus, copper-ATSM has the potential to be used to select patients who are candidates for

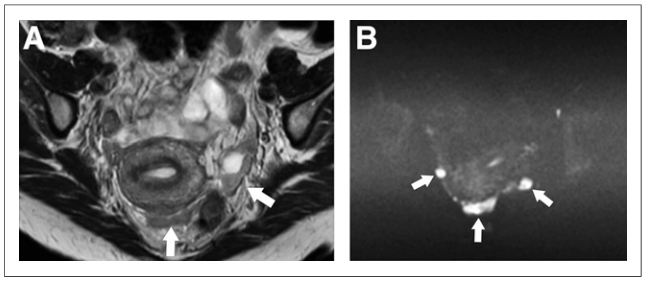

FIGURE 4. MR imaging of peritoneal carcinomatosis from ovarian cancer. Tumor nodules (arrows) are of intermediate signal intensity on axial fast spin echo T2-weighted image (A) but are much more conspicuous and bright on diffusion-weighted image (B).

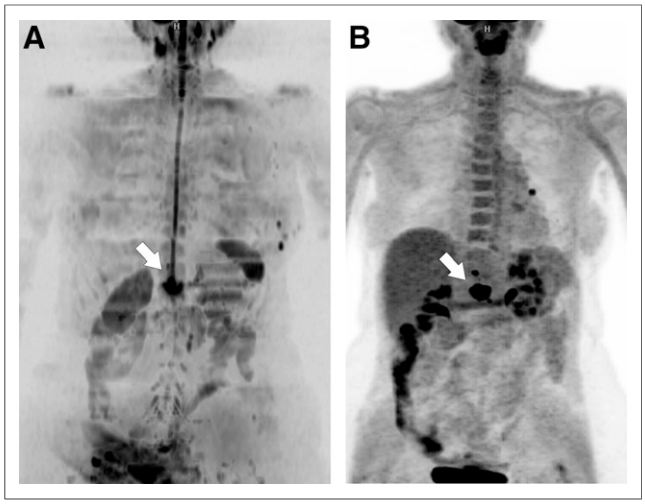

FIGURE 5. Whole-body DWI (A) and ^{18}F-FDG PET (B) images of patient with endometrial cancer recurrence in retroperitoneal node invading adjacent vertebra (arrow).

hypoxia-targeted therapy and to monitor hypoxia during such therapy.

Another tracer is 16α-^{18}F-fluoro-17β-estradiol (^{18}F-FES), an estrogen analog. ^{18}F-FES with ^{18}F-FDG has been used to image estrogen receptor expression and glucose metabolism, respectively, in endometrial lesions. Neither tracer alone could distinguish different types of endometrial lesions. However, high-risk carcinomas showed a significantly greater ^{18}F-FDG/^{18}F-FES ratio (3.6 ± 2.1) than did low-risk carcinomas (1.3 ± 0.5, $P < 0.01$) and hyperplastic lesions (0.3 ± 0.1, $P < 0.005$). Thus, ^{18}F-FDG/^{18}F-FES ratio is a noninvasive tool that differentiates among 3 histologic types of endometrial lesions (*53*).

The cell-proliferation radiotracer 3′-deoxy-3′-^{18}F-fluorothymidine (^{18}F-FLT) has been used in small clinical studies on patients with ovarian cancer. ^{18}F-FLT distributes rapidly in the extracellular fluid and is carried into the cytosol by nucleoside transporters, mainly by the equilibrative nucleoside transporter 1. Once inside the cell, ^{18}F-FLT is phosphorylated by thymidine kinase 1 and becomes trapped. Thus, the intracellular retention of ^{18}F-FLT is a measure of cellular thymidine kinase 1 activity, a principal enzyme in the salvage pathway of DNA synthesis, which is closely tied to cellular proliferation. ^{18}F-FLT uptake is higher in malignant lesions than in benign lesions (*54*). However, it remains to be proven whether ^{18}F-FLT PET/CT is specific enough to distinguish between cancerous and noncancerous tissues. The role of ^{18}F-FLT PET/CT may be in assessing and predicting response to antitumor therapy, an area in which it has been shown to be superior to ^{18}F-FDG PET/CT.

PET/MR

PET/MR scanners acquire MR and PET data either simultaneously or sequentially. In the simultaneous acquisition device (mMR Biograph; Siemens), the PET and MR scanners are housed in a single gantry, allowing for concurrent imaging of the same body region (*55*). In the sequential acquisition device (Ingenuity TF; Philips), 2 spatially separate PET and MR scanners are connected by a moving table that reduces changes in patient positioning between successive imaging events (*56*). Both devices collect

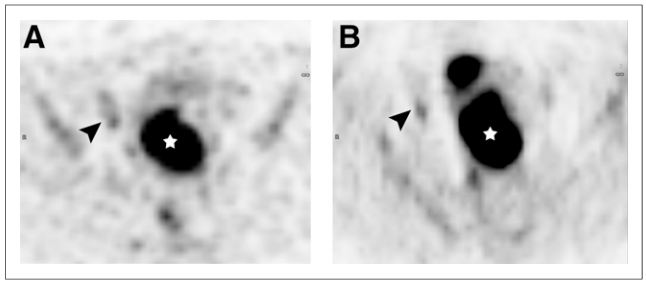

FIGURE 6. PET/MR imaging of cervical cancer with lymphadenopathy. Axial ^{18}F-FDG PET image (A) and diffusion-weighted image (B) show ^{18}F-FDG–avid and diffusion-restricted primary tumor (star) and right pelvic lymph node metastasis (arrowhead) confirmed pathologically. Node was normal by size criteria (not shown).

MR PET datasets in a single imaging session, allowing for fusion image analysis.

Although the immense technical hurdles of merging PET photodetectors and MR electromagnets have been largely addressed, PET/MR continues to face several technical challenges. Most important is how to correct for photon attenuation, as unlike with CT, MR data cannot be directly extrapolated for this purpose. Tissue decomposition using Dixon sequences back-calculates attenuation by measuring the relative amounts of fat and water. But this method cannot differentiate the signal void of air from that of bone, leading to systematic underestimation of its attenuating effects (*57*). Possible solutions include atlas-based methods that retrospectively add missing tissue information and ultra-short echo time sequences that display tissues with very short T2* (e.g., bone) (*58*). Despite the remaining technical challenges, PET/MR is emerging as an important clinical and investigative tool.

In gynecologic cancer patients, ^{18}F-FDG PET/MR protocols are intended to provide "one-stop shopping" for treatment planning. The examination assesses the locoregional extent of pelvic tumor and evaluates the entire body for nodal, peritoneal, and skeletal metastases. During the PET acquisition, whole-body Dixon images, the anatomically descriptive half-Fourier acquisition single-shot turbo spin-echo images, and fluid-sensitive inversion recovery images and DWI are coacquired in simultaneous PET/MR scanners. A dedicated pelvic MR imaging examination follows and includes dynamic intravenous gadolinium administration. Patient table times on the current scanners are long, approximately 1.0–1.5 h.

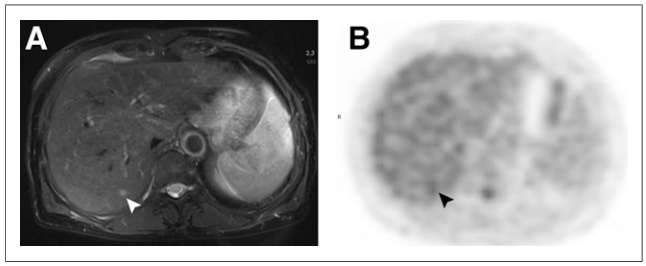

FIGURE 7. PET/MR imaging of liver metastasis from endometrial cancer. Axial T2-weighted image (A) shows 5-mm lesion (arrowhead) conspicuous on MR image but not on corresponding ^{18}F-FDG PET image (B). Lesion decreased in size with chemotherapy.

Preliminary experience is encouraging. Lesions detected on PET or DWI can be precisely localized and characterized on the conventional MR sequences, thereby allowing for improved sensitivity without a loss of specificity. These include lymph node (Fig. 6) and bone and liver (Fig. 7) metastases. Although the resolution of MR is more limited than that of CT, it nevertheless can detect lesions below the resolution of PET, such as pulmonary nodules. Finally, the parameters standarized uptake value, apparent diffusion coefficient, and tumor volume can be measured in conjunction with the imaging information for more quantitative assessment.

CONCLUSION

Pelvic MR imaging and whole-body PET/CT fill complementary roles in the imaging assessment of gynecologic cancer. MR imaging diagnoses and defines tumor extent in the central pelvic soft tissues, and PET/CT evaluates for lymphadenopathy and extrapelvic metastases. Future improvements in scanner and postprocessing technology will likely expand the role of DCE MR imaging and DWI. PET tracers other than ^{18}F-FDG will offer evaluation of tumor phenotype noninvasively. Early experience with PET/MR imaging indicates that this technique will emerge as the mainstay of tracer development and imaging assessment in gynecologic cancer patients.

REFERENCES

1. American Cancer Society. *Cancer Facts & Figures 2014.* Atlanta, Georgia: American Cancer Society; 2014.
2. Pecorelli S. Revised FIGO staging for carcinoma of the vulva, cervix, and endometrium. *Int J Gynaecol Obstet.* 2009;105:103–104.
3. Koh WJ, Greer BE, Abu-Rustum NR, et al. Cervical cancer. *J Natl Compr Canc Netw.* 2013;11:320–343.
4. Pandharipande PV, Choy G, del Carmen MG, Gazelle GS, Russell AH, Lee SI. MRI and PET/CT for triaging stage IB clinically operable cervical cancer to appropriate therapy: decision analysis to assess patient outcomes. *AJR.* 2009;192:802–814.
5. Hricak H, Gatsonis C, Chi DS, et al. Role of imaging in pretreatment evaluation of early invasive cervical cancer: results of the intergroup study American College of Radiology Imaging Network 6651—Gynecologic Oncology Group 183. *J Clin Oncol.* 2005;23:9329–9337.
6. Mitchell DG, Snyder B, Coakley F, et al. Early invasive cervical cancer: tumor delineation by magnetic resonance imaging, computed tomography, and clinical examination, verified by pathologic results, in the ACRIN 6651/GOG 183 Intergroup Study. *J Clin Oncol.* 2006;24:5687–5694.
7. Sironi S, Buda A, Picchio M, et al. Lymph node metastasis in patients with clinical early-stage cervical cancer: detection with integrated FDG PET/CT. *Radiology.* 2006;238:272–279.
8. Loft A, Berthelsen AK, Roed H, et al. The diagnostic value of PET/CT scanning in patients with cervical cancer: a prospective study. *Gynecol Oncol.* 2007;106:29–34.
9. Selman TJ, Mann C, Zamora J, Appleyard TL, Khan K. Diagnostic accuracy of tests for lymph node status in primary cervical cancer: a systematic review and meta-analysis. *CMAJ.* 2008;178:855–862.
10. Roh JW, Seo SS, Lee S, et al. Role of positron emission tomography in pretreatment lymph node staging of uterine cervical cancer: a prospective surgicopathologic correlation study. *Eur J Cancer.* 2005;41:2086–2092.
11. Lin WC, Hung YC, Yeh LS, et al. Usefulness of ^{18}F-fluorodeoxyglucose positron emission tomography to detect para-aortic lymph nodal metastasis in advanced cervical cancer with negative computed tomography findings. *Gynecol Oncol.* 2003;89:73–76.
12. Kidd EA, Siegel BA, Dehdashti F, et al. Lymph node staging by positron emission tomography in cervical cancer: relationship to prognosis. *J Clin Oncol.* 2010;28:2108–2113.
13. Lakhman Y, Akin O, Park KJ, et al. Stage IB1 cervical cancer: role of preoperative MR imaging in selection of patients for fertility-sparing radical trachelectomy. *Radiology.* 2013;269:149–158.
14. Signorelli M, Guerra L, Montanelli L, et al. Preoperative staging of cervical cancer: is 18-FDG-PET/CT really effective in patients with early stage disease? *Gynecol Oncol.* 2011;123:236–240.
15. Grigsby PW, Siegel BA, Dehdashti F, Rader J, Zoberi I. Posttherapy ^{18}F-fluorodeoxyglucose positron emission tomography in carcinoma of the cervix: response and outcome. *J Clin Oncol.* 2004;22:2167–2171.
16. Koh WJ, Greer BE, Abu-Rustum NR, et al. Uterine neoplasms, version 1.2014. *J Natl Compr Canc Netw.* 2014;12:248–280.
17. Kinkel K, Forstner R, Danza FM. Staging of endometrial cancer with MRI: guidelines of the European Society of Urogenital Imaging. *Eur Radiol.* 2009;19:1565–1574.
18. Mariani A, Dowdy SC, Cliby WA, et al. Prospective assessment of lymphatic dissemination in endometrial cancer: a paradigm shift in surgical staging. *Gynecol Oncol.* 2008;109:11–18.
19. Duncan KA, Drinkwater KJ, Frost C, Remedios D, Barter S. Staging cancer of the uterus: a national audit of MRI accuracy. *Clin Radiol.* 2012;67:523–530.
20. Antonsen SL, Jensen LN, Loft A, et al. MRI, PET/CT and ultrasound in the preoperative staging of endometrial cancer: a multicenter prospective comparative study. *Gynecol Oncol.* 2013;128:300–308.
21. Signorelli M, Guerra L, Buda A, et al. Role of the integrated FDG PET/CT in the surgical management of patients with high risk clinical early stage endometrial cancer: detection of pelvic nodal metastases. *Gynecol Oncol.* 2009;115:231–235.
22. Selman TJ, Christopher H, Mann CH, Zamora J. Khan KS. A systematic review of tests for lymph node status in primary endometrial cancer. *BMC Womens Health.* 2008;8:8.
23. Picchio M, Mangili G, Samanes Gajate AM, et al. High-grade endometrial cancer: value of [^{18}F]FDG PET/CT in preoperative staging. *Nucl Med Commun.* 2010;31:506–512.
24. Kitajima K, Murakami K, Yamasaki E, et al. Performance of FDG-PET/CT in the diagnosis of recurrent endometrial cancer. *Ann Nucl Med.* 2008;22:103–109.
25. Sironi S, Picchio M, Landoni C, et al. Post-therapy surveillance of patients with uterine cancer: value of integrated FDG PET/CT in the detection of recurrence. *Eur J Nucl Med Mol Imaging.* 2007;34:472–479.
26. Berchuck A, Anspach C, Evans AC, et al. Postsurgical surveillance of patients with FIGO stage I/II endometrial adenocarcinoma. *Gynecol Oncol.* 1995;59:20–24.
27. Kurman RJ, Shih IeM. The origin and pathogenesis of epithelial ovarian cancer: a proposed unifying theory. *Am J Surg Pathol.* 2010;34:433–443.
28. van Nagell JR Jr, DePriest PD, Ueland FR, et al. Ovarian cancer screening with annual transvaginal sonography: findings of 25,000 women screened. *Cancer.* 2007;109:1887–1896.
29. Kinkel K, Lu Y, Mehdizade A, Pelte MF, Hricak H. Indeterminate ovarian mass at US: incremental value of second imaging test for characterization—meta-analysis and Bayesian analysis. *Radiology.* 2005;236:85–94.
30. Fenchel S, Grab D, Nuessle K, et al. Asymptomatic adnexal masses: correlation of FDG PET and histopathologic findings. *Radiology.* 2002;223:780–788.
31. Mutch DG, Prat J. 2014 FIGO staging for ovarian, fallopian tube and peritoneal cancer. *Gynecol Oncol.* 2014;133:401–404.
32. Morgan RJ Jr, Alvarez RD, Armstrong DK, et al. Ovarian cancer, version 3.2012. *J Natl Compr Canc Netw.* 2012;10:1339–1349.
33. Tempany CM, Zou KH, Silverman SG, Brown DL, Kurtz AB, McNeil BJ. Staging of advanced ovarian cancer: comparison of imaging modalities—report from the Radiological Diagnostic Oncology Group. *Radiology.* 2000;215:761–767.
34. Gu P, Pan LL, Wu SQ, Sun L, Huang G. CA 125, PET alone, PET-CT, CT and MRI in diagnosing recurrent ovarian carcinoma: a systematic review and meta-analysis. *Eur J Radiol.* 2009;71:164–174.
35. Sebastian S, Lee SI, Horowitz NS, et al. PET-CT vs. CT in ovarian cancer recurrence. *Abdom Imaging.* 2008;33:112–118.
36. Tofts PS. Modeling tracer kinetics in dynamic Gd-DTPA MR imaging. *J Magn Reson Imaging.* 1997;7:91–101.
37. Seki H, Kimura M, Sakai K. Myometrial invasion of endometrial carcinoma: assessment with dynamic MR and contrast-enhanced T1-weighted images. *Clin Radiol.* 1997;52:18–23.
38. Beddy P, Moyle P, Kataoka M, et al. Evaluation of depth of myometrial invasion and overall staging in endometrial cancer: comparison of diffusion weighted and dynamic contrast-enhanced MR imaging. *Radiology.* 2012;262:530–537.
39. Mayr NA, Yuh WTC, Jajoura D, et al. Ultra-early predictive assay for treatment failure using functional magnetic resonance imaging and clinical prognostic parameters in cervical cancer. *Cancer.* 2010;116:903–912.
40. Thomassin-Naggara I, Balvay D, Aubert E, et al. Quantitative dynamic contrast-enhanced MR imaging analysis of complex adnexal masses: a preliminary study. *Eur Radiol.* 2012;22:738–745.

41. Nakamura K, Imafuku N, Nishida T, et al. Measurement of the minimum apparent diffusion coefficient (ADCmin) of the primary tumor and CA125 are predictive of disease recurrence for patients with endometrial cancer. *Gynecol Oncol.* 2012;124:335–339.
42. Fujii S, Matsusue E, Kanasaki Y, et al. Detection of peritoneal dissemination in gynecological malignancy: evaluation by diffusion-weighted MR imaging. *Eur Radiol.* 2008;18:18–23.
43. Lin G, Ng KK, Chang CJ, et al. Myometrial invasion in endometrial cancer: diagnostic accuracy of diffusion-weighted 3.0-T MR imaging—initial experience. *Radiology.* 2009;250:784–792.
44. Lin G, Ho KC, Wang JJ, et al. Detection of lymph node metastasis in cervical and uterine cancers by diffusion-weighted magnetic resonance imaging at 3T. *J Magn Reson Imaging.* 2008;28:128–135.
45. Kim JK, Kim KA, Park BW, Kim N, Cho KS. Feasibility of diffusion-weighted imaging in the differentiation of metastatic from nonmetastatic lymph nodes: early experience. *J Magn Reson Imaging.* 2008;28:714–719.
46. Nakai G, Matsuki M, Inada Y, et al. Detection and evaluation of pelvic lymph nodes in patients with gynecologic malignancies using body diffusion-weighted magnetic resonance imaging. *J Comput Assist Tomogr.* 2008;32:764–768.
47. Michielsen K, Vergote I, Op de Beeck K. MRI with diffusion-weighted sequence for staging of patients with suspected ovarian cancer: a clinical feasibility study in comparison to CT and FDG-PET/CT. *Eur Radiol.* 2014;24:889–901.
48. Höckel M, Schlenger K, Hockel S, et al. Tumor hypoxia in pelvic recurrences of cervical cancer. *Int J Cancer.* 1998;79:365–369.
49. Pitson G, Fyles A, Milosevic M, et al. Tumor size and oxygenation are independent predictors of nodal diseases in patients with cervix cancer. *Int J Radiat Oncol Biol Phys.* 2001;51:699–703.
50. Lewis JS, McCarthy DW, McCarthy TJ, et al. Evaluation of ^{64}Cu-ATSM in vitro and in vivo in a hypoxic tumor model. *J Nucl Med.* 1999;40:177–183.
51. Dehdashti F, Grigsby PW, Mintun MA, et al. Assessing tumor hypoxia in cervical cancer by positron emission tomography with ^{60}Cu-ATSM: relationship to therapeutic response—a preliminary report. *Int J Radiat Oncol Biol Phys.* 2003;55:1233–1238.
52. Dehdashti F, Grigsby PW, Lewis JS, et al. Assessing tumor hypoxia in cervical cancer by PET with ^{60}Cu-labeled diacetyl-bis(N4-methylthiosemicarbazone). *J Nucl Med.* 2008;49:201–205.
53. Tsujikawa T, Yoshida Y, Kudo T, et al. Functional images reflect aggressiveness of endometrial carcinoma: estrogen receptor expression combined with ^{18}F-FDG PET. *J Nucl Med.* 2009;50:1598–1604.
54. Richard SD, Bencherif B, Edwards RP, et al. Noninvasive assessment of cell proliferation in ovarian cancer using ^{18}F-3′deoxy-3-fluorothymidine positron emission tomography/computed tomography imaging. *Nucl Med Biol.* 2011; 38:485–491.
55. Delso G, Furst S, Jakoby B, et al. Performance measurements of the Siemens mMR integrated whole-body PET/MR scanner. *J Nucl Med.* 2011;52:1914–1922.
56. Zaidi H, Ojha N, Morich M, et al. Design and performance evaluation of a whole-body Ingenuity TF PET-MRI system. *Phys Med Biol.* 2011;56:3091–3106.
57. Catana C, Guimaraes AR, Rosen BR. PET and MR imaging: the odd couple or a match made in heaven? *J Nucl Med.* 2013;54:815–824.
58. Quick HH. Integrated PET/MR. *J Magn Reson Imaging.* 2014;39:243–258.

JNM The Journal of NUCLEAR MEDICINE

Evaluation of Gynecologic Cancer with MR Imaging, ^{18}F-FDG PET/CT, and PET/MR Imaging

Susanna I. Lee, Onofrio A. Catalano and Farrokh Dehdashti

J Nucl Med. 2015;56:436-443.
Published online: January 29, 2015.
Doi: 10.2967/jnumed.114.145011

The Journal of Nuclear Medicine is published monthly.
SNMMI | Society of Nuclear Medicine and Molecular Imaging
1850 Samuel Morse Drive, Reston, VA 20190.
(Print ISSN: 0161-5505, Online ISSN: 2159-662X)

SNMMI SOCIETY OF NUCLEAR MEDICINE AND MOLECULAR IMAGING